Him. Phys. **14** 45-56, (2026) ISSN: 2542-2545

Himalayan Physics

An examination of the spin vector orientation of r-magnitude SDSS DR-15 galaxies within the redshift range of 0.50 to 0.60

https://doi.org/10.3126/hp.v14i1.92569

Dhan Singh Dhami[1], Bishnu Bist[1], Shiv Narayan Yadav[2*], Birendra Prasad Yadav[2]

1 Department of Physics, Patan Multiple Campus, Lalitpur, Tribhuvan University, Nepal

2 Central Department of Physics, Tribhuvan University, Nepal

Abstract: This study explores the spatial orientations of a large sample of 483,899 galaxies selected from the SDSS DR-15 catalog with redshifts ranging from 0.50 to 0.60. The primary objective is to examine the spin vector orientations of these galaxies in the context of three galaxy evolution models: the Pancake Model, the Hierarchy Model, and the Primordial Vorticity Model. To achieve this, the observed two-dimensional parameters, including celestial coordinates, position angles, and inclination angles, are transformed into three-dimensional spin vector orientations, represented by the polar and azimuthal angles, using the Flin–Godłowski transformation. Expected isotropic distribution curves are generated by accounting for selection biases through Monte Carlo simulations of 10^7 virtual galaxies. The observed and expected distributions are then compared using three statistical tests: the chi-square test, autocorrelation analysis, and Fourier analysis. The dataset is divided into 17 distinct samples for detailed investigation. The results predominantly support the Hierarchy Model, while a few samples exhibit signatures consistent with the Primordial Vorticity Model. The analysis is carried out in the equatorial coordinate system, and local effects are identified through graphical features such as humps and dips in the angular distributions.

Keywords: Galaxies • Redshift • Galaxies evolution model • Orientation

Received: 2026-04-04 **Revised: 2026-06-27** **Published: 2026-08-17**

I. Introduction

The universe originated with the Big Bang and has been expanding and cooling ever since. During the earliest moments of its evolution, the universe was extremely hot and dense, creating physical conditions that are difficult to reproduce or fully comprehend. The major stages of cosmic evolution can be summarized as follows. From the Big Bang until approximately 10^{-6} s, particle physics dominated the evolution of the universe. During this period, the temperature was so high that the conventional laws of physics, including the behavior of the fundamental forces, differed significantly from those observed today.

* *Corresponding Author: shiva.yadav@cdp.tu.edu.np*

Experimental studies using high-energy particle accelerators provide valuable insights into these extreme conditions. Approximately one second after the Big Bang, the universe cooled sufficiently for subatomic particles to combine and form the lightest elements, primarily hydrogen. About 380,000 years later, the temperature decreased enough for stable hydrogen atoms to form, marking the epoch of recombination. The abundance of hydrogen observed in the present universe provides strong evidence supporting the Big Bang theory. According to Gamow [1], density fluctuations generated during the inflationary epoch played a crucial role in the formation of cosmic structures and addressed several shortcomings of the classical Big Bang model.

The formation and evolution of galaxies are strongly influenced by their angular momentum and rotational properties [2]. The origin of galaxy spin vectors is closely related to their spatial orientations, which provide important information about the gravitational instability responsible for the formation of large-scale structures [3]. Studies of galaxy orientations primarily focus on determining the direction of the spin vector with respect to a chosen reference plane. The observed distributions are then compared with theoretically expected isotropic distributions using various statistical techniques and numerical simulations.

The analysis of galaxy spin vectors provides valuable information about the distribution of angular momentum within galaxy clusters and superclusters, thereby offering insights into the early stages of galaxy and cluster formation, assuming that the angular momentum of galaxies has remained approximately conserved throughout their evolution. Previous investigations have examined the preferred alignment of angular momentum vectors of SDSS galaxies in the Coma Cluster using the position angle–inclination method [4, 5] in the Equatorial Coordinate System (ECS), Galactic Coordinate System (GCS), and Supergalactic Coordinate System (SGCS). Such studies have contributed significantly to understanding the evolutionary history of galaxy clusters.

Galaxy Evolution Models

Several theories have been proposed to explain the origin and evolution of galaxies and large-scale structures in the universe. Among them, the most widely discussed models include the Hierarchy Model, Pancake Model, Primordial Vorticity Model, Li Model, and Ostriker Model. Although all of these models are based on cosmological principles, they predict significantly different distributions of galaxy angular momentum vectors.

The Pancake Model [6, 7] predicts that the angular momentum vectors of galaxies preferentially align parallel to the reference plane (Fig. 1). According to this model, large-scale structures formed first as massive gaseous "pancakes," which subsequently fragmented into galaxies through adiabatic instabilities. The model is based on the gravitational instability scenario, in which the amplification of small primordial density perturbations leads to the formation of thin, dense gaseous sheets.

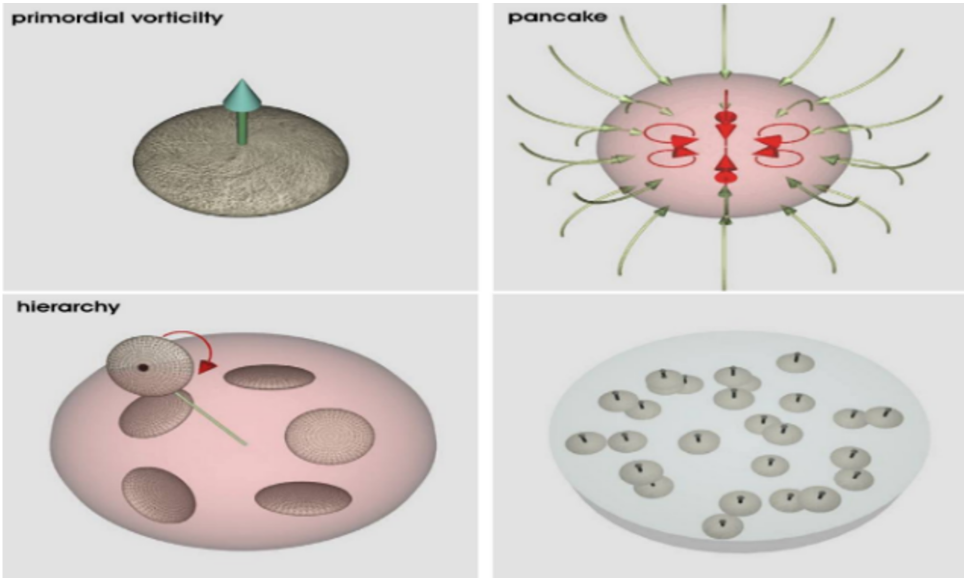

Figure 1. Schematic illustration of the preferred orientation of galaxy angular momentum vectors predicted by different galaxy evolution models [8].

In contrast, the Hierarchy Model [3] predicts that the angular momentum vectors of galaxies should exhibit a random orientation with respect to the reference plane. In this scenario, galaxies form first and subsequently acquire angular momentum through tidal interactions during hierarchical clustering. They continue to evolve through mergers of protogalactic clouds or already formed galaxies [9]. Consequently, the model predicts an isotropic distribution of galaxy spin vectors within large-scale structures. Spatial orientations of galaxies in 112 galaxy clusters have been investigated under this framework [10–19].

Previous studies have reported a systematic variation in galaxy alignments from early-type (BM I) to late-type (BM III) clusters [14, 20]. These results suggest that spiral-rich (late-type) clusters (BM II–III and BM III) exhibit stronger preferred alignments than elliptical-rich (early-type) clusters [21].

The Primordial Vorticity Model [22, 23] predicts that galaxy angular momentum vectors are preferentially oriented perpendicular to the reference plane. According to this model, a dynamically rotating proto-cluster first develops due to primordial cosmic vorticity in the early universe. Subsequent density and pressure fluctuations then trigger the formation of galaxies. For this reason, the model is often referred to as the top-down scenario.

In the present study, we analyze SDSS galaxies using the r-magnitude catalog. The SDSS r band corresponds to the red portion of the optical spectrum and is centered at approximately 6165 Å. The photometric observations were obtained using the CCD imaging system mounted on the SDSS 2.5-m telescope at Apache Point Observatory, New Mexico, USA. The r band is particularly suitable for tracing stellar populations and galaxy morphology and is widely used in studies of galaxy evolution. The primary objective is to examine the spin vector orientations of these galaxies in the context of three galaxy evolution models: the Pancake Model, the Hierarchy Model, and the Primordial Vorticity Model.

II. Methods and Materials

Flin–Godłowski Transformation

The orientation of a galaxy spin vector is described by two parameters: the polar angle (θ) and the azimuthal angle (ϕ). The detailed derivation of these angles was presented by Flin and Godłowski [4]. The values of θ and ϕ are obtained from the observable quantities in the Equatorial Coordinate System (ECS), as given in Eqs. 1 and 2.

$$\sin\theta = -\cos i\,\sin\delta \pm \sin i\,\sin P\,\cos\delta \tag{1}$$

$$\sin\phi = (\cos\theta)^{-1}\left[-\cos i\,\cos\delta\,\sin\alpha + \sin i\,(\mp\sin P\,\sin\delta\,\sin\alpha \mp \cos P\,\cos\alpha)\right] \tag{2}$$

where i is the inclination angle, while α, δ, and P represent the right ascension, declination, and position angle, respectively. The inclination angle is calculated using

$$\cos^2 i = \frac{q^2 - q^{*2}}{1 - q^{*2}}, \tag{3}$$

which is valid for oblate spheroids [9]. Here, q and q^* denote the observed axial ratio (b/a) and the intrinsic flatness of a galaxy, respectively.

Selection Effects

Selection effects in the observational database significantly influence the expected isotropic distribution curves. To minimize these effects, isotropic distribution curves were generated through Monte Carlo simulations using 10^7 virtual galaxies [24]. The values of θ and ϕ were calculated using the Flin–Godłowski transformation described in Eqs. 1 and 2. The simulated galaxies were generated using the observed distributions of α, δ, P, and i. The input files required for the simulations were prepared using MATLAB R2015a.

Analytical Techniques

The observed galaxy distributions were compared with the expected isotropic distributions for both the θ and ϕ angle distributions using three statistical methods: the chi-square test, the Fourier test, and the autocorrelation test.

Chi-square Test

The chi-square (χ^2) test is widely used to compare the observed distribution with the expected distribution under a given hypothesis. It provides a quantitative measure of the goodness of fit between the observed and expected isotropic distributions. The reduced chi-square and chi-square statistics are expressed as

$$\chi^2_\nu = \frac{\chi^2}{\nu}, \tag{4}$$

$$\chi^2 = \sum_{i=1}^{n} \frac{(N_{Oi} - N_{Ei})^2}{N_{Ei}}, \tag{5}$$

where n is the number of angular bins, N_{Oi} and N_{Ei} denote the observed and expected isotropic frequencies, respectively, and $\nu = n - 1$ is the degree of freedom [11].

Fourier Test

The Fourier test is applicable for detecting slowly varying deviations from isotropy in the θ or ϕ distributions. The first-order Fourier coefficients are given by

$$\Delta_{11} = \frac{\sum_{k=1}^{n} (N_k - N_{0k}) \cos 2\theta_k}{\sum_{k=1}^{n} N_{0k} \cos^2 2\theta_k}, \tag{6}$$

$$\Delta_{21} = \frac{\sum_{k=1}^{n} (N_k - N_{0k}) \sin 2\theta_k}{\sum_{k=1}^{n} N_{0k} \sin^2 2\theta_k}. \tag{7}$$

The corresponding standard deviations are

$$\sigma(\Delta_{11}) = \left(\sum_{k=1}^{n} N_{0k} \cos^2 2\theta_k \right)^{-1/2}, \tag{8}$$

$$\sigma(\Delta_{21}) = \left(\sum_{k=1}^{n} N_{0k} \sin^2 2\theta_k \right)^{-1/2}. \tag{9}$$

The amplitude of the first-order Fourier coefficient is defined as

$$\Delta_1 = \left(\Delta_{11}^2 + \Delta_{21}^2 \right)^{1/2}, \tag{10}$$

and the corresponding first-order Fourier probability is

$$P(>\Delta_1) = \exp\left(-\frac{nN_0\Delta_1^2}{4}\right), \tag{11}$$

with the standard deviation

$$\sigma(\Delta_1) = \left(\frac{2}{nN_0}\right)^{1/2}. \tag{12}$$

The coefficient Δ_{11} is particularly important because it measures the deviation from isotropy. A statistically significant value of Δ_{11} indicates the presence of a preferred alignment of galaxy spin vectors with respect to the reference plane [11].

Autocorrelation Test

The autocorrelation test is used to detect correlations between the numbers of galaxies in adjacent angular bins. The autocorrelation coefficient is given by

$$C = \sum_{k=1}^{n} \frac{(N_k - N_{0k})(N_{k+1} - N_{0,k+1})}{\sqrt{N_{0k}N_{0,k+1}}}, \tag{13}$$

with the corresponding standard deviation

$$\sigma(C) = \sqrt{n}. \tag{14}$$

For an isotropic distribution, no correlation is expected, and therefore the autocorrelation coefficient approaches zero ($C \to 0$) [11].

III. Results and Discussion

An anisotropic distribution is identified when the chi-square probability satisfies $P(<\chi^2) < 0.050$, the autocorrelation coefficient is greater than 1.0 or less than -1.0, the normalized first-order Fourier coefficient $\Delta_{11}/\sigma(\Delta_{11})$ is greater than 1.5 or less than -1.5, and the first-order Fourier probability satisfies $P(>\Delta_1) < 0.150$ [25].

Local effects in the galaxy samples are interpreted in terms of crests and troughs in the angular distributions. A significant negative value of $\Delta_{11}/\sigma(\Delta_{11})$ for the θ distribution indicates that the galaxy spin vectors preferentially orient perpendicular to the reference coordinate plane, whereas a significant positive value indicates a preferential parallel alignment. In the θ-distribution histograms, where the observed data are represented by solid circles with $\pm 1.5\sigma$ error bars, a hump in the range $0° \leq \theta < 45°$ indicates that the angular momentum vectors tend to align parallel to the equatorial plane, whereas a hump in the range $45° \leq \theta \leq 90°$ indicates a preferential perpendicular orientation [20].

For the ϕ distribution, a significant positive value of $\Delta_{11}/\sigma(\Delta_{11})$ suggests that the projected angular momentum vectors tend to point toward the centre of the Equatorial Coordinate System, whereas a significant negative value indicates a preferentially tangential orientation [20]. Interpreting humps and dips in the ϕ-distribution histograms is comparatively more complex, because the azimuthal angle ranges from $-90°$ to $+90°$ [10, 11]. Since the projected vectors point radially toward the centre of the coordinate system when $\phi = 0°$, a hump in the central ten bins indicates a radial orientation of the projected spin vectors, whereas humps in the first and last four bins indicate a preferentially tangential orientation [5].

Table 1 summarizes the statistical parameters obtained for the polar angle (θ) distribution of all 17 samples. Applying the criteria above, samples r01, r02, r06, r08, r09, and r10 display statistically significant anisotropy, while the remaining eleven samples (r03, r04, r05, r07, r11–r17) are consistent with an isotropic θ distribution. Sample r03 is representative of the isotropic group: its statistical values are $P(>\chi^2) = 0.376$, $C/C(\sigma) = 0.1$, $\Delta_{11}/\sigma(\Delta_{11}) = -0.8$, and $P(>\Delta_1) = 0.547$, all four of which satisfy the isotropy criteria.

Table 1. Statistical parameters for the polar angle (θ) distribution.

Sample	$P(>\chi^2)$	$C/C(\sigma)$	$\Delta_{11}/\sigma(\Delta_{11})$	$P(>\Delta_1)$
r01	0.010	4.2	-2.6	0.021
r02	0.000	8.5	-3.5	0.001
r03	0.376	0.1	-0.8	0.547
r04	0.427	-0.2	0.0	0.726
r05	0.342	0.5	-1.0	0.505
r06	0.225	2.3	-1.6	0.096
r07	0.089	0.7	-1.3	0.261
r08	0.002	2.7	-2.8	0.003
r09	0.063	1.7	-2.5	0.011
r10	0.133	0.8	-1.7	0.121
r11	0.209	0.2	-0.4	0.603
r12	0.234	-2.6	0.7	0.761
r13	0.863	0.0	-0.3	0.903
r14	0.487	-0.7	-0.6	0.763
r15	0.972	0.0	-0.1	0.945
r16	0.509	0.0	0.6	0.638
r17	0.010	-2.3	-0.1	0.986

Table 2 presents the corresponding statistics for the azimuthal angle (ϕ) distribution. In contrast to Table 1, the chi-square probabilities for samples r05–r14 are all well below 0.05, accompanied by large autocorrelation and Fourier coefficients, indicating pronounced anisotropy in ϕ even for several samples whose θ distribution is isotropic. This contrast between the two angle distributions is examined further below.

Fig. 2 illustrates the θ and ϕ distributions for sample r03, chosen as a representative isotropic case. In the small-angle region ($\theta \leq 45°$, Fig. 2(a)), the observed and expected numbers of galaxies are 1926 and 1941, respectively – a deficit of only 15 galaxies – while in the large-angle region ($\theta \geq 45°$) the observed number (626) exceeds the expected number (611) by the same margin. No significant humps or dips appear in either region, consistent with the randomly oriented, isotropic θ distribution reported in Table 1.

Table 2. Statistical parameters for the azimuthal angle (ϕ) distribution.

Sample	$P(>\chi^2)$	$C/C(\sigma)$	$\Delta_{11}/\sigma(\Delta_{11})$	$P(>\Delta_1)$
r01	0.547	1.6	-0.6	0.147
r02	0.234	1.1	-0.8	0.211
r03	0.486	0.4	1.9	0.114
r04	0.193	-0.1	2.1	0.077
r05	0.000	6.1	5.1	0.001
r06	0.002	13.6	7.8	0.009
r07	0.001	25.5	11.4	0.109
r08	0.000	43.0	14.7	0.014
r09	0.003	50.1	16.1	0.002
r10	0.001	50.9	14.7	0.008
r11	0.001	38.4	11.9	0.118
r12	0.008	25.4	8.6	0.110
r13	0.005	9.4	5.7	0.007
r14	0.002	3.3	3.3	0.008
r15	0.289	-0.6	0.5	0.822
r16	0.755	0.4	0.0	0.972
r17	0.876	0.0	1.1	0.512

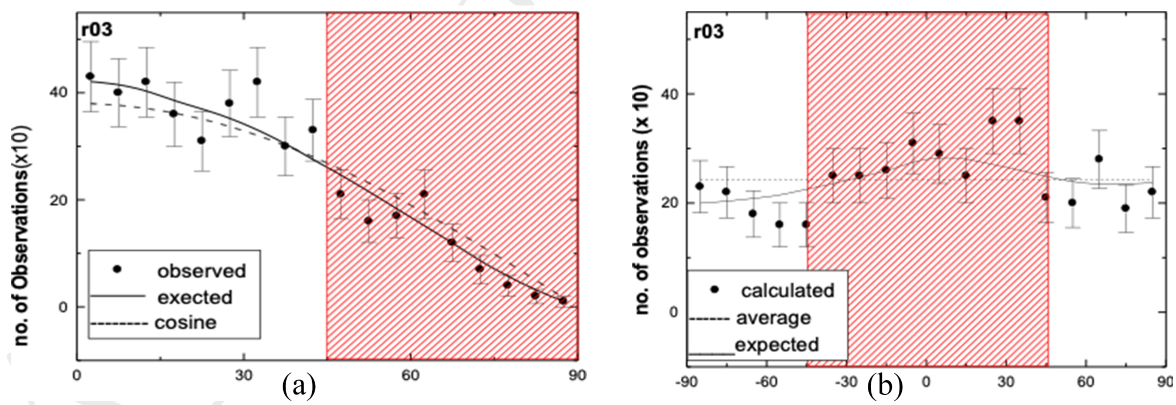

Figure 2. Distributions of (a) Polar angle (θ), and (b) Azimuthal angle (ϕ) galaxies for sample r03. The solid curve represents the expected isotropic distribution, while the dashed curve denotes the cosine distribution for the polar angle and the average distribution for the azimuthal angle. The observed counts are shown with $\pm 1.5\sigma$ statistical error bars.

For the azimuthal angle (Fig. 2(b)), the statistical parameters listed in Table 2 are $P(>\chi^2) = 0.486$, $C/C(\sigma) = 0.4$, $\Delta_{11}/\sigma(\Delta_{11}) = 1.9$, and $P(>\Delta_1) = 0.114$. The observed and expected numbers of galaxies in the central ten bins are 1787 and 1734, respectively – an excess of 53 observed galaxies – whereas the expected counts exceed the observed counts by 28 and 25 galaxies in the first four and last four bins, respectively. No statistically significant humps or dips are present. The slightly positive first-order Fourier coefficient suggests a weak tendency for the projected spin vectors to point toward the centre of the Equatorial Coordinate System, although the overall ϕ distribution remains close to isotropic. This isotropic behaviour in both θ and ϕ is also seen in samples r04, r05, r07, r11, r12, r13, r14, r15, r16, and r17.

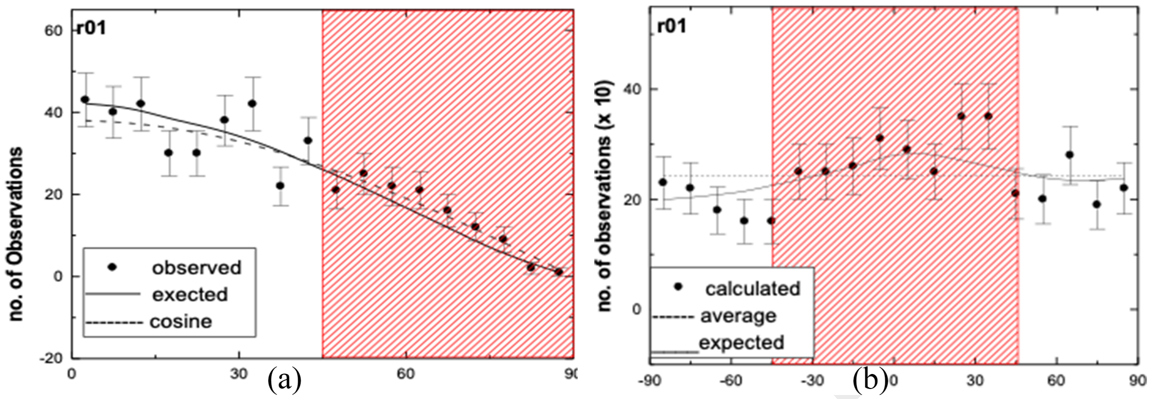

Figure 3. Distributions of (a) Polar angle (θ), and (b) Azimuthal angle (ϕ) galaxies for sample r01. The solid curve represents the expected isotropic distribution, while the dashed curve denotes the cosine distribution for the polar angle and the average distribution for the azimuthal angle. The observed counts are shown with $\pm 1.5\sigma$ statistical error bars.

In contrast, Fig. 3 presents the θ and ϕ distributions for sample r01, chosen as a representative anisotropic case. Table 1 gives $P(>\chi^2) = 0.010$, $C/C(\sigma) = 4.2$, $\Delta_{11}/\sigma(\Delta_{11}) = -2.6$, and $P(>\Delta_1) = 0.021$ for the polar angle distribution; all four statistics indicate a significant deviation from isotropy. In the small-angle region (Fig. 3(a)), the observed and expected numbers of galaxies are 307 and 365, respectively. Although no prominent hump is observed, continuous dips are present at 17.5°, 22.5°, and 37.5°. In the large-angle region, the observed number (146) exceeds the expected number (88) by 58 galaxies, with continuous humps at 52.5°, 57.5°, 62.5°, 67.5°, 72.5°, and 77.5°. Both the statistical tests and the graphical analysis therefore indicate that the spin vectors of sample r01 are preferentially oriented perpendicular to the reference plane, in agreement with the Primordial Vorticity Model. The same anisotropic behaviour is observed in samples r02, r06, r08, r09, and r10.

The azimuthal angle distribution of sample r01, however, is close to isotropic: $P(>\chi^2) = 0.547$, $C/C(\sigma) = 1.6$, $\Delta_{11}/\sigma(\Delta_{11}) = -0.6$, and $P(>\Delta_1) = 0.147$ (Table 2). As shown in Fig. 3(b), the observed and expected numbers of galaxies in the central ten bins are identical (223 galaxies), and the expected counts exceed the observed counts by only two galaxies in the first four and last four bins, with no significant humps or dips. Except for the autocorrelation coefficient, all statistical tests thus indicate an isotropic ϕ distribution for r01, the opposite of its anisotropic θ distribution. This contrast suggests that the inferred alignment may depend on the choice of reference coordinate system; further analyses using the Galactic and Supergalactic Coordinate Systems are therefore required to verify it [26].

IV. Conclusions

In this study, we investigated the spatial orientations of 483,899 SDSS DR-15 galaxies with redshifts ranging from 0.50 to 0.60 using the Equatorial Coordinate System as the reference frame. The position angle–inclination method proposed by Flin and Godłowski was employed to transform the observed two-dimensional parameters into three-dimensional galaxy spin vectors. To account for observational selection effects, isotropic reference distributions were generated through Monte Carlo simulations of 10^7 virtual galaxies. The observed and simulated distributions were compared using the chi-square, autocorrelation, and Fourier statistical tests. The main conclusions are summarized as follows.

1. Samples r03, r04, r05, r07, r11, r12, r13, r14, r15, r16, and r17 exhibit random spin-vector orientations, supporting the Hierarchy Model of galaxy formation and evolution [3].

2. Samples r01, r02, r06, r08, r09, and r10 show statistically significant anisotropy in their polar angle distributions. The negative values of the normalized first-order Fourier coefficient indicate that the galaxy spin vectors preferentially orient perpendicular to the reference plane, supporting the Primordial Vorticity Model [22, 23].

3. Several samples exhibit different behaviours in the θ and ϕ distributions. This discrepancy suggests that the inferred alignment may depend on the adopted reference coordinate system. Further analyses using the Galactic Coordinate System and the Supergalactic Coordinate System are therefore required.

4. Monte Carlo simulations of 10^7 virtual galaxies were successfully performed. The resulting isotropic distributions are smooth and agree well with the theoretical expectations.

5. Localized deviations from isotropy are observed in a few samples, including r03, r07, r09, r12, and r17. These local effects may arise from tidal torquing or gravitational lensing during the evolution of large-scale structures.

V. Acknowledgements

The authors would like to thank the Central Department of Physics, Tribhuvan University, Dr. Ajay Kumar Jha, Dr. Kishori Yadav, Prof. Dr. Narayan Prasad Adhikari, Mr. D. N. Chaudhary and Sloan Digital Sky Surveys (SDSS).

References

[1] Gamow G. The role of turbulence in the evolution of the universe. Phys Rev. 1952;86:251-60.

[2] von Weizsacker CF. The evolution of galaxies and stars. Astrophys J. 1951;114:165-86.

[3] Peebles PJE. Origin of the angular momentum of galaxies. Astrophys J. 1969;155:393-401.

[4] Flin P, Godłowski W. The orientation of galaxies in the local supercluster. Mon Not R Astron Soc. 1986;222:525-41.

[5] Yadav SN. A Study of z-Magnitude Dependence in the Spatial Orientation of Angular Momentum Vectors of Galaxies having Redshift < 30,000 km s^{-1}. Tribhuvan University Journal. 2016;30(2):195-210.

[6] Doroshkevich AG. The origin of rotation of galaxies. Astrophys J. 1973;14:11-3.

[7] Doroshkevich AG, Shandarin SF, Saar E. Spatial structure of protoclusters and the formation of galaxies. Mon Not R Astron Soc. 1978;184:643-60.

[8] Kausch W. A statistical approach to a possible alignment of galaxies in the Perseus cluster; 2004. M.Sc. dissertation, Innsbruck University.

[9] Holmberg E. On the apparent diameters and the orientation in space of extragalactic nebulae. Meddelanden fran Lunds Astronomiska Observatorium Series II. 1946;117:3-82.

[10] Godłowski W. Galactic orientation within the local supercluster. Mon Not R Astron Soc. 1993;265:874-80.

[11] Godłowski W. Some aspects of the galactic orientation within the local supercluster. Mon Not R Astron Soc. 1994;271:19-30.

[12] Flin P. The anisotropy of galaxy orientation in the Coma/A1367 supercluster. Mon Not R Astron Soc. 2001;325:49-58.

[13] Aryal B, Kandel S, Saurer W. Spatial orientation of galaxies in the core of the Shapley concentration – the cluster Abell. Astron Astrophys J. 2006;458:357-67.

[14] Aryal B, Paudel S, Saurer W. Spatial orientations of galaxies in seven Abell clusters of BM type II. Mon Not R Astron Soc. 2007;379:1011-21.

[15] Aryal B, Kafle PR, Saurer W. Radial velocity dependence in the spatial orientations of galaxies in and around the local Supercluster. Mon Not R Astron Soc. 2008;389:741-9.

[16] Aryal B, Neupane D, Saurer W. Morphological dependence in the spatial orientations of galaxies around the Local Supercluster. Astrophys Space Sci. 2008;314:177-86.

[17] Aryal B, Paudel S, Saurer W. Coexistence of chiral symmetry restoration and random orientation of galaxies. Astron Astrophys J. 2008;479:397-407.

[18] Aryal B, Yadav SN, Saurer W. Spatial orientation of galaxies in the Zone of Avoidance. Bull Astron Soc India. 2012;40:65-76.

[19] Aryal B, Bhattarai H, Dhakal S, Rajbahak C, Saurer W. Spatial orientation of angular momentum vectors of galaxies in six rotating clusters. Mon Not R Astron Soc. 2013;434:1939-51.

[20] Yadav SN, Aryal B. Preferred alignments of angular momentum vectors of galaxies in six dynamically

unstable Abell clusters. Res Astron Astrophys. 2017;17(7):064.

[21] Yadav SN, Sah SK. Study of Spatial Orientation of Angular Momentum of z-Magnitude SDSS DR-13 Galaxies with Red Shift 0.50 to 0.53. J Inst Sci Technol. 2021;26(1):1-7.

[22] Ozernoy LM. Dynamical parameters of galaxy clusters as a consequence of cosmological turbulence. Soviet Astronomy. 1971;15:923-33.

[23] Stein R. Galaxy formation from primordial turbulence. Astron Astrophys J. 1974;35:17-29.

[24] Aryal B, Saurer W. Comments on the expected isotropic distribution curves in galaxy orientation studies. Astron Astrophys. 2000;364:L97-L100.

[25] Yadav SN, Aryal B. A Study of r- and u-Magnitude Dependence in the Spatial Orientation of Spin Vectors of SDSS Galaxies having redshift 0.10 < z < 0.11. Himalayan Phys. 2014;5:1-11.

[26] Godłowski W. Remarks on the methods of investigations of alignment of galaxies. Astrophys J. 2012;747(1):7.